

AN INVESTIGATION OF SOME PHYSICOMECHANICAL CHARACTERISTICS ASSOCIATED WITH THE PERFORATION OF A BARRIER

Yu. S. Stepanov

Zhurnal Prikladnoi Mekhaniki i Tekhnicheskoi Fiziki, No. 3, pp. 111-114, 1966

**ABSTRACT:** The results of experiments to determine some of the parameters characterizing the perforation of a barrier made of a series of materials are set forth. These include the momentum imparted to the barrier when it is perforated, the diameters of the holes, the angles of front and rear dispersion, and a number of others.

1. Let us consider the case of deliberate perforation of a barrier of thickness  $t$  by a particle. We shall introduce the coefficients

$$k = \frac{m_2}{m_0 + \Delta P}, \quad \beta = \frac{J_1}{J_0}, \quad v = \frac{\varepsilon_1}{E_0}. \quad (1.1)$$

Here  $m_2$  is the mass penetrating behind the barrier at velocity  $v_2$ ,  $m_0$  is the mass of the particle,  $\Delta P$  is the mass lost by the barrier when it is perforated,  $J_1$  is the momentum imparted to the barrier due to perforation,  $J_0$  and  $E_0$  are the initial momentum and the energy of the particle,  $\varepsilon_1$  is that part of the energy converted to heat and irreversible volume strains behind the plastic wave. Thus, the coefficient  $k$  determines that part of the mass having the velocity  $v_2$  behind the barrier, the coefficient  $\beta$  that part of the momentum received by the barrier. The equations for momentum and mass are written in the form

$$J_0(1 - \beta) = m_2v_2 - m_3v_3, \\ J_0 = m_0v_0, \quad m_0 + \Delta P = m_2 + m_3. \quad (1.2)$$

Here  $v_0$  is the velocity of the particle,  $m_3$  is the mass detached in the direction opposite to the direction of impact with velocity  $v_3$ . If the process of perforation is determined by the mechanism set forth previously in [1, 2], then the equation of conservation of mass up to commencement of forcing out of the "plug" [1] is written in the form

$$m_0v_0^2 = (m_1 + m_0)v_1^2 + 2\varepsilon_1, \quad m_0v_0 = (m_1 + m_0)v_1. \quad (1.3)$$

Here  $m_1$  is the mass of the barrier participating in the inelastic impact ( $m_1 > \Delta P$ ) and moving at velocity  $v_1$  behind the plastic wave in the barrier up to the time it leaves the rear surface of the barrier. From this

$$v = 1 - \frac{m_0}{m_0 + m_1}. \quad (1.4)$$

2. The powder system and the light-gas ballistic apparatus employed in [3] were used to accelerate compact spherical particles. The impact velocity did not exceed 3.5 kg/sec. The barriers were made of Mark D-16T duralumin, Mark ST-3 steel, brass, cadium, tin, zinc, lead, Mark P-500 polyethylene, porolon, sponge rubber, RK-9 rubber, polyethylene terephthalate (PETF), Mark ST glass-reinforced textolite, polyisobutylene rubber, butyl rubber, and Mark SKB synthetic rubber.

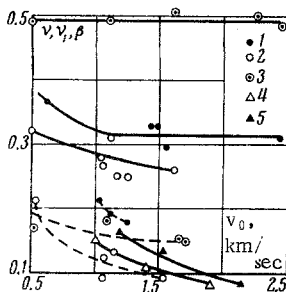


Fig. 1

The accelerated particles were made of the same metals. Steel particles were used for impact against barriers made of polymer materials. In all cases, the spheres had a diameter  $d_0$  of 10 mm.

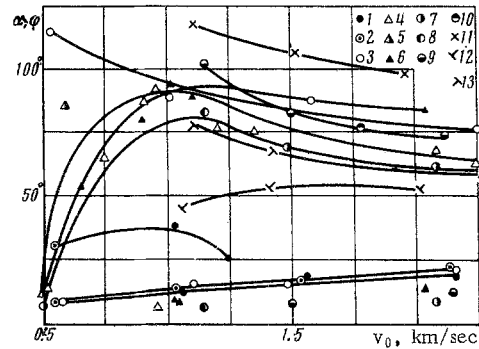


Fig. 2

Electronic chronometers of the "Neptun" type were used to measure the velocities  $v_0$  and  $v_2$ ; they received electric signals from wire sensors, and the velocities were determined on two bases for measurement [3]. The quantity  $\Delta P$  increased with growth in  $l$  with  $v_0 = \text{const}$  and  $\rho_1 = \text{const}$  ( $\rho_1$  is the density of the barrier), and with growth in  $\rho_1$  with  $v_0 = \text{const}$  and  $l = \text{const}$ . The coefficients of the linear relationship  $v_2 = a(v_0 - b)$  are given in the table. It can be seen that the velocity  $v_2$  dropped for a given  $v_0$  with increasing  $l$  and  $\rho_1$ .

As can be seen in the table, in a number of cases  $d_0 \approx l$ , thus one can consider with sufficient accuracy that the mass  $m_2$  flies out distributed with distance, but with a velocity  $v_2$  close to constant. This is also substantiated by the experiments described in reference [2]. It was noted in the experiments that there was a punched-out part of the barrier were distributed in the rear dispersion cone.

In order to determine the coefficient  $k$  from (1.1), experiments were conducted in the following manner: a semi-infinite barrier made of material with a known relationship of the reactive momentum coefficient  $\xi(v_0)$  was installed behind the thin barrier of the material under study [3]. The distance between barriers was chosen so that the entire mass  $m_2$  was intercepted by a semi-infinite barrier installed on a ballistic pendulum. Then,  $m_2$  was determined from the equation

$$\xi(v_2) = J_R [(m_1' + m_2)(m_2v_2^2 - 2Q)]^{-1/2}, \quad J_R = J_n - m_2v_2. \quad (2.1)$$

Here,  $J_R$  is the reactive momentum,  $m_1'$  is the mass ejected from the crater in the semi-infinite barrier,  $J_n$  is the experimentally measured total momentum transmitted to the barrier, and  $Q$  are the losses of energy to latent heats of phase transformation [1, 3]. The value of  $m_2$  was determined in check measurements by weighing the sheets of rubber (traps) placed behind the barrier to be studied. It follows from calculations of  $k$  by the experimentally obtained mass  $m_2$  that with through perforation, there is no back scattering up to  $v_0 \sim 1$  km/sec ( $k = 1$ ). Then,  $k$  decreases, and for velocities  $v_0 \sim 3$  to 4 km/sec, it tends toward 0.5 ( $m_3 \approx m_2$ ). It should be noted that no back scattering was ever noted for polyethylene, porolon, or rubbers, including RK-9 rubber.

In the case of through perforation, a part of the momentum of the particle  $J_1$  was received by the remaining barrier. In order to determine  $J_1$ , it was attached to a ballistic pendulum so that the particle would fly on through without hindrance after penetrating it, and the pendulum fixed the momentum  $J_1$ . If there were no back scattering, then, according to (1.2),

$$J_0 = m_2v_2 + J_1. \quad (2.2)$$

Experimentally,  $v_3 \sim 0.05 v_0$  [4], which substantiates (2.2). Then, both  $\beta$  and  $m_2$  can be determined from these experiments. The values

of  $k$  obtained in this manner agreed satisfactorily with previously determined values. The relationship  $\alpha(v_0)$  also decreasing with growth in  $v_0$  tended toward values much less than one. Thus, henceforth we can neglect the value of  $\beta$  for high velocities  $v_0$ .

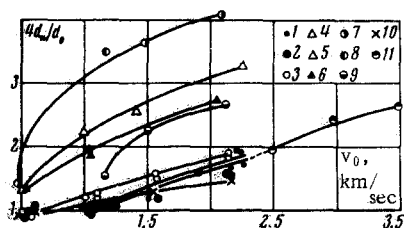


Fig. 3

In order to determine the coefficient  $\nu$  by (1.4), sections of the holes in the barriers were made and the mass involved in irreversible strains was found by weighing. The sum of this mass and  $\Delta P$  yielded the value of  $m_1$ . It is interesting to compute the coefficient  $\nu_1$  defining the part of the energy  $E_0$  dissociated into heat in the front of the shock wave. The value of  $\nu_1$  is calculated by the known equation of state of the materials in the particle and the barrier, taking the cubic attenuation of pressure at the front of the shock wave into a consideration [1]. Sections of the holes and craters were constructed on a large scale for the conducted experiments for graphical representation of the pressure drop at the front of the shock wave in the particle and the barrier. The drops  $T(x)$  (where  $T$  is the temperature at the front of the shock wave) corresponding to the pressure drop at the front  $p(x)$  ( $x$  is the coordinate) made it possible to compute the share of the thermal component of internal energy and, consequently,  $\nu_1$ .

The data on  $\nu$ ,  $\nu_1$ , and  $\beta$  for Fe and D16T are plotted in Fig. 1. The following notation is used there  $\alpha(v_0)$ : 1) Fe  $\rightarrow$  D16T,  $l = 1.0$  cm; 2) Fe  $\rightarrow$  D16T,  $l = 0.5$  cm; 3) Fe  $\rightarrow$  Fe,  $l = 0.5$  cm,  $\alpha(v_0)$ ; 4) Fe  $\rightarrow$  D16T,  $l = 0.5$  cm; 5) Fe  $\rightarrow$  D16T,  $l = 1.0$  cm. In this case, the dashed lines show the relationship  $\nu_1(v_0)$ . It can be seen that  $\nu_1$  increases with growth of the density and the thickness of the barrier,  $\beta$  with growth of the thickness of the barrier with  $v_0 = \text{const}$ . The increase in  $\nu$  and  $\nu_1$  with the thickness of the barrier can be explained qualitatively by the greater amount of heated mass. Averaging the values of  $\nu$  due to scatter of the data is explained by inaccuracies the experimental determination of  $m_1$ . The share of the energy  $E_0$  transmitted to the barrier was also determined experimentally by a calorimetric method for semi-infinite targets of Fe, Al, Cd, Sn, and Pb. Its ratio to  $E_0$  drops with increased  $v_0$ , which can be explained qualitatively by the increase in energy carried off by the mass  $m_3$  ejected from the crater. The problem of the diameter of the ejected part of the barrier ("plug") is important. Experiments involving through perforation showed that the hole in the barrier most often has the shape of a hyperboloid of revolution of one sheet, and a part of the material is sometimes carried off in face and rear fragments. One can assume that the "plug" has a cylindrical shape and is ejected before the total hole is formed. The shape of the hole (hyperboloid of revolution) is probably formed from the interaction of the sections of the hemispherical shock wave reflected from the rear surface and those still arriving. Thus, it is necessary to take the diameter of the "plug" as the minimum diameter of the hole  $d_*$ .

3. It is of interest to determine the dependence of the angles of rear ( $\varphi$ ) and face ( $\alpha$ ) dispersion during perforation on various factors.

For this purpose, sheets of Whatman paper were placed in front of and behind the target in order to fix the field of flight of small fragments. The results are presented in Fig. 2. The following notation is used: 1) Fe  $\rightarrow$  D16T,  $l = 1.0$  cm; 2) Fe  $\rightarrow$  D16T,  $l = 0.5$  cm; 3) Fe  $\rightarrow$  Fe,  $l = 0.5$  cm; 4) Cd  $\rightarrow$  Cd; 5) Fe  $\rightarrow$  Cd; 6) Sn  $\rightarrow$  Sn; 7) Fe  $\rightarrow$  Pb; 8) Pb  $\rightarrow$  Pb; 9) Zn  $\rightarrow$  Zn; 10) Fe  $\rightarrow$  Zn; 11) Fe  $\rightarrow$  sponge rubber; 12) Fe  $\rightarrow$  NETF; 13) Fe  $\rightarrow$  ST.

As a result of these experiments, one can draw the following conclusions in regard to angles  $\varphi$  and  $\alpha$ : 1) no dependence of angles  $\varphi$  and  $\alpha$  on  $l$  could be found as the data for different  $l$  lay well on the relationship  $\alpha(v_0)$  and  $\varphi(v_0)$  for one pair; 2)  $\varphi$  and  $\alpha$  did not depend on the density of the particle  $\rho_0$  (agreement of the relationships  $\varphi_7$  and  $\varphi_8$ ,  $\alpha_7$  and  $\alpha_8$ ,  $\alpha_4$  and  $\alpha_5$ , and others); 3) when  $l = \text{const}$ , the angles  $\varphi$  and  $\alpha$  increased with increasing density of the barrier  $\rho_1$ ; 4)  $\varphi$  increases slightly with increasing  $v_0$ ; 5) the relationship  $\alpha(v_0)$  has a clearly marked maximum at  $v_0 \sim 1.0$  km/sec which is followed by a slight decrease; 6) the value  $\varphi \sim 20^\circ$  to  $25^\circ$ ,  $\alpha \sim 60^\circ$  to  $120^\circ$ . The relationship 7 by  $(v_0)$  has a value of about  $60^\circ$  when  $v_0 \sim 3.1$  km/sec is not shown in Fig. 2. The experiments showed that the face fragments (angle  $\alpha$ ) were distributed in a narrow zone at the side surface of the circular dispersion cone and the rear fragments covered the dispersion field almost evenly. It can be assumed that the annular dispersion of the face fragments is due to the introduced particle and the decrease in relationship  $\alpha(v_0)$  following the maximum begins after the particle is broken into fragments.

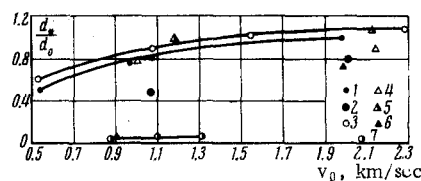


Fig. 4

Figure 3 shows the relationships  $d_*(v_0)/d_0$  for metals. The notation corresponds to the notation of Fig. 2 with the following exceptions: 10) Fe  $\rightarrow$  brass,  $l = 0.2$  cm; 11) Fe  $\rightarrow$  6061-T6,  $l = 0.475$  cm. The relationship 11 is taken from [5] for a steel sphere  $d_0 = 0.63$  cm and Mark 6061-T6 duralumin. It can be seen that the relationship 2 obtained in this work joins satisfactorily with relationship 11 at higher impact velocities  $v_0$ . Figure 4 shows the experimental data for  $d_*(v_0)/d_0$  for polymer materials. The following notation is employed: 1) Fe  $\rightarrow$  polyethylene,  $l = 1.0$  cm; 2) Fe  $\rightarrow$  PETF,  $l = 0.5$  cm; 3) Fe  $\rightarrow$  polyethylene,  $l = 0.1$  cm; 4) Fe  $\rightarrow$  PETF,  $l = 0.2$  cm; 5) Fe  $\rightarrow$  PETF,  $l = 12 \cdot 10^{-4}$  cm; 6) Fe  $\rightarrow$  sponge rubber,  $l = 5.0$  cm; 7) Fe  $\rightarrow$  RK-9 rubber,  $l = 2.5$  cm. In some cases (for example, butyl rubber and polyisobutylene) the hole was observed to be completely filled in [9]. On the basis of the relationships of Figs. 3 and 4, one can conclude that the ratio  $d_*/d_0$  with  $v_0 = \text{const}$  increases in the case of metals with increased density of the barrier  $\rho_1$ , thickness of the barrier  $l$ , and particle density  $\rho_0$  (for the given range of velocities). At the same time, we observe an inverse pattern in the polymers;  $d_*$  decreases with increasing  $l$  even though the diameter of the perforation increases on the level of the initial and rear surfaces. One may assume that when  $l$  increases, the time for forming the hole increases and, consequently, the time for maintaining some temperature of local heating in the annular zone about the hole, which is essential to the process of filling in holes in polymers. As a consequence of this, the internal diameter

	$l$ , cm	$a$	$b$ , km/sec		$l$ , cm	$a$	$b$ , km/sec
Fe $\rightarrow$ D16T	0.5	1	0.14	Fe $\rightarrow$ polyethylene	0.1	1	0.03
Fe $\rightarrow$ D16T	1.0	0.89	0.18	Fe $\rightarrow$ porolon	3.85	1	0.03
Fe $\rightarrow$ Fe	0.5	0.666	0.18	Fe $\rightarrow$ sponge rubber	4.5	1	0.15
Fe $\rightarrow$ brass	0.2	0.9	0.14	Fe $\rightarrow$ RK-9 rubber	2.03	0.82	0.05
Cd $\rightarrow$ Cd	1.15	0.652	0.67	Fe $\rightarrow$ PETF	0.2	1	0.03
Sn $\rightarrow$ Sn	2.0	0.267	0.3	Fe $\rightarrow$ PETF	12.10 <sup>-4</sup>	1	0.03
Zn $\rightarrow$ Zn	1.49	0.555	0.85	Fe $\rightarrow$ glass reinforced textolite	0.5	0.9	0.05
Fe(Fb) $\rightarrow$ Pb	0.97	0.55	0.2	Fe $\rightarrow$ polyisobutylene	3.6	1	0.2
Fe $\rightarrow$ polyethylene	0.99	1	0.05	Fe $\rightarrow$ butyl rubber	4.42	0.785	0

$d_*$  decreases, even though the outer diameter of the perforation increases with growth in  $l$ . We also note that when  $l = \text{const}$  with increasing  $d_0$ , this  $l = l_1$  (for the accepted  $v_0$ ) and  $d_* = \max d_* (l_1$  is the maximum depth of penetration). For larger  $v_0$  with the same  $d_0 = \text{const}$ , this is  $l < l_1$  and  $d_* < \max d_*$ . Thus, the relationship  $d_*(v_0)/d_0$  may be convex upwards, which is substantiated by experimental data (Fig. 3).

The author thanks V. P. Potreba for his help with the experiments and E. I. Andriankin for discussing the work.

## REFERENCES

1. E. I. Andriankin and Yu. S. Stepanov, "Depth of penetration resulting from the impact of meteoric particles," collection: Artificial Earth Satellites [in Russian], no. 15, p. 44, Izd-vo AN SSSR, 1963.

2. R. F. Recht, T. W. Ipson, "Ballistic perforation dynamics," J. Appl. Mech., vol. 30, no. 3, p. 384, 1963.

3. B. A. Arkhipov and Yu. S. Stepanov, "Momentum calculations in crater formation and the modeling of impact processes," PMTF [Journal of Applied Mechanics and Technical Physics], no. 3, p. 120, 1965.

4. L. V. Belyakov, V. P. Valitskii, and N. A. Zlatin, "The role of thermal phenomena in the impact of metal bodies," DAN SSSR, vol. 160, no. 2, 1965.

17 June 1965

Moscow